PAPER

Check for updates

Short-chain fluorocarbon-based polymeric coating with excellent nonwetting ability against chemical warfare agents†

Hyunsook Jung, *[a] Jihyun Kwon,[a] Heesoo Jung,*[a] Kyeong Min Cho, [a] Seung Jung Yu,[a] Sang Myeon Lee,[a] Mingyu Jeon[b] and Sung Gap Im [b]

The ongoing concerns and regulations on long-chain fluorinated compounds (C8 or higher) for nonwetting coatings have driven the market to search for sustainable alternative chemistries. In this study, a copolymeric coating containing short-chain fluorinated groups was synthesized to achieve excellent nonwetting ability against hazardous chemical warfare agents (CWAs). A copolymer of 1H,1H,2H,2H-perfluorooctyl methacrylate (PFOMA) and ethylene glycol dimethacrylate (EGDMA, crosslinker) was directly coated onto a textile fabric *via* initiated chemical vapor deposition. The p(PFOMA-*co*-EGDMA) coating shows a rough-textured morphology with a bumpy, raspberry-like structure leading to high contact angles ($\theta_{water} > 150°$ and $\theta_{dodecane} = 113.8°$) and a small water shedding angle (<5°). Moreover, the p(PFOMA-*co*-EGDMA) coating was further analysed for application in military fabrics: air permeability, tensile strength, and safety against toxic perfluorooctanoic acid (PFOA) and perfluorooctanesulfonic acid (PFOS). Outstanding nonwetting was noticeably achieved against different CWAs, including bis(2-chloroethyl)sulfide (HD), pinacolyl methylfluorophosphonate (GD), and O-ethyl S-(2-diisopropylaminoethyl)methylphosphonothioate (VX) ($\theta_{HD} = 119.1°$, $\theta_{GD} = 117.0°$, and $\theta_{VX} = 104.1°$). The coating retained its nano-structuration and nonwetting ability for water and n-dodecane despite being subjected to 250 cycles of Martindale abrasion and harsh chemicals (NaOH and HCl). The robustness and scalable straightforward preparation route of the coating make it an ideal approach for designing durable next-generation CWA nonwetting coatings for fabrics with favorable health and environmental properties.

1. Introduction

On a battlefield, the likelihood of military personnel being exposed to hazardous chemicals, such as chemical warfare agents (CWAs) as well as everyday substances, including water, oils, fuel, lubricants, and cleaners, is considerably high. CWAs, such as bis(2-chloroethyl) sulfide (HD) and nerve agents, including pinacolyl methylfluorophosphonate (GD) and O-ethyl S-(2-diisopropylaminoethyl) methylphosphonothioate (VX), are classified as highly lethal chemical weapons.[1] These chemicals are mostly present in liquid form and have low volatility, which can be potentially dangerous to the soldiers. Traditionally, long-chain (C8) fluorocarbon-based coatings have been applied to military fabrics due to their ability to repel a wide range of

liquids ranging from high surface tension water to low surface tension oils.[2–4] Indeed, the (C8) fluorocarbon coatings have helped to reduce the adsorption of toxic chemicals on the outer layer fabric of soldiers, thus drastically reducing the permeation of toxic chemicals through clothing and effectively keeping them safe in a contaminated environment.[5] However, C8-coated clothing loses its efficacy after repeated laundering and exposure to harsh weather elements, which is a grave concern to military clients.[6] Furthermore, the C8-based long perfluorooctyl pendant groups have been criticized for containing residual raw precursors and trace levels of perfluoroalkyl acids as impurities.[7] The residual materials and the product themselves may degrade to form toxic perfluorooctanoic acid (PFOA) and perfluorooctanesulfonic acid (PFOS), which have been shown to have a long half-life in wildlife and humans.[8] Therefore, regulatory actions have been put in place or are being considered in several countries to manage these chemicals. For instance, within the European Union (EU), PFOS is regulated to the detectable levels of 1 μg m^{-2} in textile fabrics and the limits for PFOA are currently under discussion.[9] In the USA., PFOA was banned for use in 2015 by the Environmental Protection Agency.[10]

[a] Chem-Bio Technology Center, Agency for Defense Development, Yuseong-gu, Daejeon 34063, Republic of Korea. E-mail: junghs@add.re.kr; hsjung@add.re.kr

[b] Department of Chemical & Biomolecular Engineering, Korea Advanced Institute of Science and Technology (KAIST), 291 Daehak-ro, Yuseong-gu, Daejeon 34131, Republic of Korea

† Electronic supplementary information (ESI) available. See DOI: 10.1039/d1ra08326k

Recently, there has been a shift within industries toward green chemistries. One promising shift has been to replace long-chain (C8) fluorocarbons with short-chain (C6) fluorocarbons in the coatings for favorable health and environmental properties.[11–14] The short-chain fluorocarbons are less toxic and have a lower bioaccumulation potential compared to long-chain fluorocarbons.[11] Indeed, due to shorter chain and lower number of fluorine groups, the repellency performance of C6 coatings is reduced to a narrower range of liquids. Nevertheless, (C6) fluorocarbon-based coatings have been reported to possess as good water repellency as C8-based coatings, and some commercially available C6-based coatings even exhibit omniphobic behavior.[12,15] Recently, a novel coating based on C6 fluorocarbons and silica nanoparticles has been developed,[5,16] which, when applied to military fabrics, resulted in higher durability than the currently used C8 coating and an effective nonwetting against oils and certain organic solvents. However, there remains the challenge of repelling very low surface tension and polar liquids, such as the nerve agent, GD.[17]

A significant amount of research has been reported on water-repellent fabrics.[18–24] By contrast, CWAs are toxic and relatively uncommon, and therefore, studies on coatings with an ability to repel CWAs are relatively scarce. We recently reported an omniphobic textile surface that repels both water ($\theta_{water} > 150°$) and liquid HD ($\theta_{HD} = 107°$) by combining a zirconium-based porous metal–organic framework (MOF) and a polyhedral oligomeric silsesquioxane (POSS).[20] We also demonstrated PFOA-free fluoropolymer-coated silica nanoparticles (Si NPs) coatings, exhibiting large CAs ($\theta_{water} = 154°$, $\theta_{dodecane} = 121°$, $\theta_{HD} = 129°$, $\theta_{GD} = 72°$, and $\theta_{VX} = 87°$).[25]

Herein, we present a polymeric coating with C6 fluorinated short side-chains that exhibits an excellent nonwetting ability toward a variety of chemical warfare agents, including HD, GD, and VX. A copolymer of perfluorooctyl methacrylate (PFOMA, C6, monomer) and ethylene glycol dimethacrylate (EGDMA, crosslinker) was directly coated onto a nylon/cotton (50/50) fabric via initiated chemical vapor deposition (iCVD). The iCVD technique allows the direct synthesis of polymeric layers at the interface to achieve durable conformal coating with well-defined chemical composition over a large area and virtually no surface or substrate limitations.[26–28] PFOMA is particularly appealing for nonwetting surfaces applications, as it combines the hydrophobic properties of the short-chain (C6) fluorinated pendant groups with easy processability. EGDMA, a low-viscosity diester with no free hydrophilic groups, offers high cross-link density and flexibility in various polymer applications.[29,30] The results showed that the iCVD-prepared PFOMA copolymeric coating had a rough-textured surface feature on the fabric and exhibited an outstanding nonwetting ability against CWAs, such as HD, GD, and VX as well as water and *n*-dodecane. Moreover, the coating retained its nonwetting ability even after mechanical abrasion and harsh chemical corrosion.

2. Experimental

2.1. Materials and reagents

The initiator *tert*-butyl peroxide (TBPO) (98%, Aldrich), the monomer precursor 1*H*,1*H*,2*H*,2*H*-perfluorooctyl methacrylate (PFOMA) (Tokyo Chemical Industry), and the crosslinker ethylene glycol dimethacrylate (EGDMA) (98%, Aldrich) were used as received without further purification. Nylon/cotton (50/50) fabric was kindly provided by the Korea Textile Development Institute.

2.2. Preparation of polymeric coatings by iCVD

Poly(1*H*,1*H*,2*H*,2*H*-perfluorooctyl methacrylate-*co*-ethylene glycol dimethacrylate) or p(PFOMA-*co*-EGDMA) was directly synthesized on the fabric (200 mm × 150 mm). Typically, PFOMA, EGDMA, and TBPO were heated to 70, 90, and 25 °C, respectively. Vaporized PFOMA, EGDMA, and TBPO flowed into a custom-built iCVD chamber, where the TBPO initiator underwent activation by heated (120 °C) filament wires placed 2 cm above the substrate. The flow rates of PFOMA, EGDMA, and TBPO were maintained at 0.26, 0.01, and 0.16 sccm, respectively, and the chamber pressure was maintained at 40 mTorr by a throttle valve during the entire process. The substrate temperature (20 °C) was controlled via a back-cooling recirculation water system. The control samples with poly(1*H*,1*H*,2*H*,2*H*-perfluorooctyl methacrylate) (p(PFOMA)) and poly(ethylene glycol dimethacrylate) (p(EGDMA)) were synthesized in a similar manner. For the preparation of p(PFOMA) coating, no EGDMA was introduced into the iCVD chamber and *vice versa* for p(EGDMA) coating.

2.3. Characterization

Scanning electron microscopy (SEM) (JSM-IT500HR, JEOL, Japan) was operated at an accelerated voltage of 5 kV and a probe current of 35 A. Atomic force microscopy (AFM) analysis was performed using a scanning probe microscope (XE-100, Park Systems, Korea). Attenuated total reflection-Fourier transform infrared spectroscopy (ATR-FTIR) measurements were taken on a Nicolet iS50 FTIR spectrometer (ThermoFisher scientific, USA). X-ray photoelectron spectroscopy (XPS) spectra were obtained with a SIGMA PROBE spectrometer (Axis Supra, Kratos, UK) using an aluminum anode (Al Kα = 1486.6 eV) operating at 75 W with a background pressure of 10^{-9} Torr. The takeoff angle was 54.7° relative to the surface normal, corresponding to a probe depth of ∼10 nm.

The p(PFOMA-*co*-EGDMA) coating fabric was further analysed by Korea Apparel Testing & Research Institute for the application to military fabrics. The air permeability of the fabric (total area of 20 cm^2) was measured with an air permeability tester (DL-3013, Daelim Starlet Co., Ltd, Siheung, Korea) at a pressure of 125 Pa. The tensile strength of the fabric (150 × 100 mm) was measured with a universal testing machine (UTM, INSTRON-5965, Instron Corporation, Canton, MA, USA). The crosshead speed is 50 mm min^{-1} and the length between the jaws was 75 mm. For safety, the p(PFOMA-*co*-EGDMA) coated fabric was analysed if there are the residual amounts of PFOA and PFOS present.

2.4. Wetting properties experiments

Wetting properties were evaluated by static contact angle (CA) and shedding angle measurements. For CA measurements, the

sessile drop method was used on a drop shape analyzer (DSA 100, KRUSS, Germany) at room temperature. In brief, a 5 μL droplet for water (deionized) and n-dodecane, and 3 μL droplets for liquid CWAs (HD, GD, and VX) were dropped from a height of 1 cm onto the sample surface in the vertical direction, and the static CAs were measured after standing for 30 s. Each liquid was tested on at least three different locations on three different coated samples.

For the water shedding angle measurement,[31] a 13 μL droplet of water was dropped (10 mm distance of needle-substrate) and onto the inclined sample surface, and the minimum angle at which the droplet of water rolled off was measured, using a USB microscope (UM12, ViTiny, USA) with an angle-adjustable manual stage (G1-80R87, DPIN).

2.5. Martindale abrasion resistance experiments

Abrasion resistance tests were performed using a Martindale Abrasion Tester (HY0401E, Huayi Science and Technology, China) at a load of 595 g. The test samples (38 mm in diameter) were rubbed against the abradant (140 mm in diameter) in the form of a geometrical pattern, following the ASTM D4966-12 standard.[32] Each rotation of the substrate was counted as one abrasion cycle with a total of 250 cycles.

2.6. Chemical corrosion resistance experiments

To assess chemical corrosion resistance, the coated fabrics were exposed to 1 M hydrochloric acid (HCl) and 1 M sodium hydroxide (NaOH) solutions under stirring (400 rpm). The samples were periodically removed, rinsed, and dried for CA and FTIR analyses.

3. Results and discussion

3.1. Preparation of polymeric coatings via iCVD

The schematic of the iCVD coating process is illustrated in Fig. 1. The iCVD chamber was held at vacuum levels, typically between 0.01 and 0.1 torr. An array of resistively heated filament wires inside the chamber causes the thermal decomposition of the initiator molecules to form free radicals.[33] A relatively modest filament temperature of 120 °C was used in the present study. Vapors of PFOMA (monomer), EGDMA (crosslinker), and TBPO (initiator) were directed into the vacuum chamber where they mixed. The free radical polymerization proceeded via a heterogeneous surface reaction between the impinging

volatile initiator radicals with adsorbed monomer and cross-linker on the substrate.[28] The copolymerization of the PFOMA and EGDMA occurred through their vinyl bonds ($\rangle C{=}CH_2$). Crosslinked polymer networks were formed by the free radical polymerization of EGDMA, and a small amount of the cross-linker was found to be effective. Notably, a limited degree of crosslinking is typically desired for increasing the average mesh size of the crosslinked network.[29] Moreover, using a low fraction of crosslinker allows the properties of the copolymer film to closely align with those of the homopolymer grown from the monovinyl monomer.[34] In control samples, the homopolymers, denoted as p(PFOMA) and p(EGDMA), were prepared in the absence of either EGDMA or PFOMA, respectively. All polymer coatings had a thickness of approximately 1000 nm, which was determined based on pre-evaluation, and provided the best conditions for the iCVD setup in terms of preparation times (deposition rates were 15 nm min^{-1}) and the final coating performance.

3.2. Characterization of polymeric coatings

As shown in Fig. 2, the SEM images depict the surface morphologies of p(PFOMA-co-EGDMA). The images show the conformal step coverage of polymeric coatings with a high degree of uniformity over a large area (up to 200 mm × 150 mm) of the fabric, which is due to the surface-growth characteristics of the iCVD process. Notably, the surface morphology of p(PFOMA-co-EGDMA) exhibited a surprising structure, consisting of a uniform layer with clusters of small spherical aggregates, forming a rasp-berry-like structure (Fig. 2a and b). The diameter of these aggregates was approximately between 500 and 1000 nm, indicating a nanostructured surface (Fig. 2c and d). By contrast, without EGDMA in the feed, the p(PFOMA) coating left the underlying surface mostly unaffected and no changes in morphology were observed (Fig. 3a and b). A more detailed look (Fig. 3b) revealed a featureless smoothly coated surface, as compared to the surfaces with p(EGDMA) coating or uncoated, which were slightly coarser (Fig. 3c–f). Previously, a copolymeric
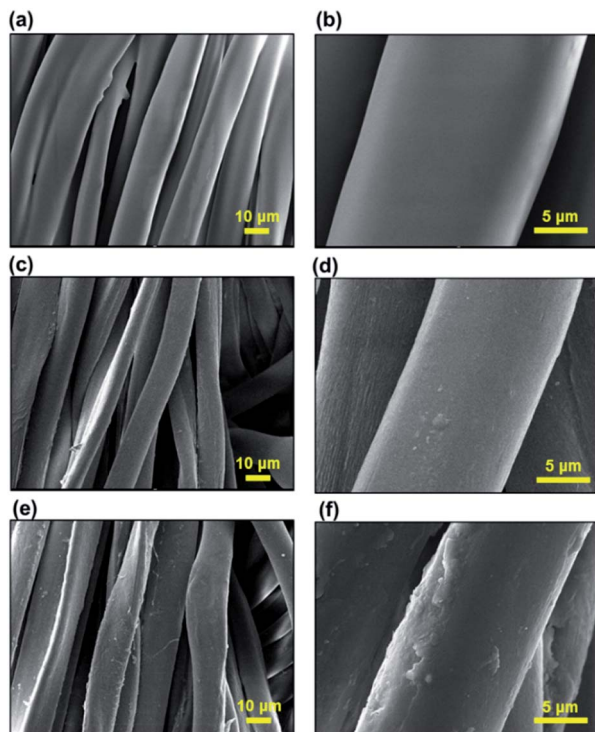

Fig. 1 Preparation of polymeric coatings via iCVD process.

Fig. 2 SEM images (a) and (b), AFM image (c) and line profile (d) of the p(PFOMA-co-EGDMA) coating.

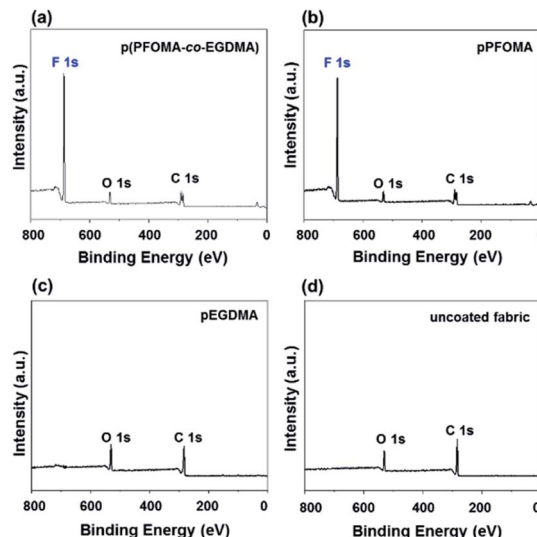Fig. 3 SEM images of polymeric coatings, (a) and (b) p(PFOMA), (c) and (d) p(EGDMA), and (e) and (f) uncoated fabric.

Fig. 4 XPS spectra of polymeric coatings of (a) p(PFOMA-*co*-EGDMA), (b) p(PFOMA), (c) p(EGDMA) coatings, and (d) uncoated fabric.

coating of 1*H*,1*H*,2*H*,2*H*-perfluorodecyl acrylate-ethylene glycol diacrylate (p(PFDA-*co*-EGDA)) with a unique nanoworm-like structure was reported.[35] It was noted that a preferential nucleation-growth of the fluorinated monomer may have induced these structures. It is certain that EGDA or EGDMA crosslinkers are crucial for the formation of such nanostructures. However, further research is required to validate their role, which is outside the scope of this study.

The chemical nature of the coatings was evaluated in detail by XPS and ATR-FTIR spectroscopy. The XPS spectra indicated the presence of C, O, and F in the coating (Fig. 4a–d). Element F existed only on the p(PFOMA-*co*-EGDMA)- and p(PFOMA)-coated surfaces (Fig. 4a and b). Obviously, F was not detected on the p(EGDMA)-coated and uncoated fabric surfaces (Fig. 4c and d). It is noteworthy that the ratios of F/C observed for the p(PFOMA-*co*-EGDMA) and p(PFOMA) were 1.08 and 1.10, respectively, indicating that the incorporation of the EGDMA between the polymeric chains did not affect the amount of F in p(PFOMA-*co*-EGDMA).

The spectra of uncoated fabric, p(PFOMA-*co*-EGDMA), p(PFOMA), and p(EGDMA) are presented in Fig. S1.† The peaks between 1146 and 1240 cm^{-1} were assigned to the asymmetric and symmetric stretching of the –CF$_2$– moiety, and the sharp peak at 1153 cm^{-1} belonged to the –CF$_2$–CF$_3$ end group.[36] These characteristic peaks attributed to PFOMA were distinctly visible in the spectrum of the p(PFOMA-*co*-EGDMA), indicating that the p(PFOMA-*co*-EGDMA) coating retained the CF$_2$ and CF$_3$ moieties originating from the monomer. The characteristic peaks for EGDMA, at 1257 and 1158 cm^{-1} were masked in the case of

p(PFOMA-*co*-EGDMA) due to the high intensity of the fluorinated segment, and thus could not be clearly distinguished. The peak centered at 1730 cm^{-1} stemmed from the C=O stretching vibration of the ester groups of both PFOMA and EGDMA.[30] Upon crosslinking, the intensity of this peak slightly increased as EGDMA has twice the C=O groups compared to PFOMA.

3.3. Wetting properties

Wetting properties were evaluated by the static CAs and water shedding angle as described in the Experimental. Particularly, in water shedding angle measurements, a drop of water (13 μL) is released onto the inclined substrate (coated fabric) from a defined height (10 mm). The minimum angle of inclination at which the drop completely rolls off the surface is determined as water shedding angle.[37] This method is more relevant to describe the CWAs behaviour in the field. Moreover, shedding angles have proven to be better suited to evaluate the wetting properties of textiles than the methods presently in use.[37]

The copolymeric coating, p(PFOMA-*co*-EGDMA) was developed with nonwetting ability against the CWAs as the goal. It is challenging to repel CWAs because of their polarity and low surface tension (γ): HD (γ = 43.2 mN m^{-1} at 20 °C), GD (γ = 24.5 mN m^{-1} at 26.5 °C), and VX (γ = 32.01 mN m^{-1} at 20 °C).[6] As wettability of a surface is usually reflected by the CAs of water and oil on it, water (γ = 72.8 mN m^{-1}, 20 °C)[38] and *n*-dodecane (γ = 28.7 mN m^{-1}, 20 °C) were also chosen as probe liquids. Fig. 5 shows the optical microscope images of various liquid droplets on the coated surfaces. Both p(PFOMA-*co*-EGDMA) and p(PFOMA) coatings exhibited extraordinary nonwetting ability against the water with θ_{water} = 152.9° and 147.1°, respectively (Fig. 5a and f). Moreover, very small water shedding angles (5° and 7° for p(PFOMA-*co*-EGDMA) and p(PFOMA), respectively) were obtained (Fig. S2†). In comparison to p(PFOMA), the p(PFOMA-*co*-EGDMA) coating exhibited a minor increase in the static CAs of water. However, an apparent increase of ∼16° in
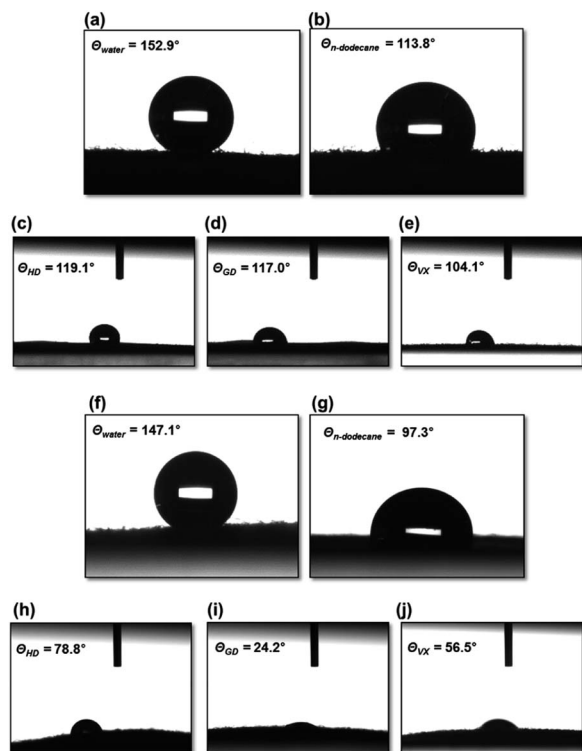
Fig. 5 Optical microscopy images and CA values of various kinds of liquids: (a) water, (b) *n*-dodecane, (c) HD, (d) GD, and (e) VX droplets onto p(PFOMA–*co*-EGDMA) coating. (f) Water, (g) *n*-dodecane, (h) HD, (i) GD, and (j) VX droplets onto p(PFOMA) coating.

the static CAs of *n*-dodecane droplets ($\theta_{n\text{-dodecane}} = 113.8°$ and $97.3°$ for p(PFOMA-*co*-EDGMA) and p(PFOMA) coating, respectively) was noticed (Fig. 5b and g).

In comparison to p(PFDMA, 3,3,4,4,5,5,6,6,7,7,8,8,9,9,10,10,10-heptadecafluorodecylmethacrylate, C8) coating by the iCVD process, where $\theta_{water} = 158°$ and $\theta_{n\text{-dodecane}} = 150°$,[39] the p(PFOMA-*co*-EGDMA) coating showed an equivalent super-omniphobic property for water only. More importantly, the static CAs were enhanced dramatically when the coated samples were exposed to CWAs (Fig. 5c–e and h–j): $\theta_{HD} = 119.1°$, $\theta_{GD} = 117.0°$, and $\theta_{VX} = 104.1°$ for the p(PFOMA-*co*-EGDMA) coating and $\theta_{HD} = 78.8°$, $\theta_{GD} = 24.2°$, and $\theta_{VX} = 56.5°$ for the p(PFOMA) coating, respectively. In comparison, the C8-based coating presently in use exhibited the CA values of $\theta_{HD} = 99.3°$ and $\theta_{GD} = 83.5°$, respectively (unofficial data). It should be noted that the static CAs of HD, GD, and VX are still less than 150°, which is not a standard superomniphobic value.[38,39] Indeed, it was observed that the droplets of HD, GD, and VX penetrate into the porous, coated fabric materials. This phenomenon occurred within 5 min for GD droplet, showing the rapid decrease in the static CAs (Fig. S3†). However, the static CAs of HD droplet scarcely changed during the CAs measurements which continued up to 240 min (Fig. S3†).

Reportedly, roughened surface structures tend to decrease the wettability of a surface.[38] With a specific structure, roughness alone can impart super-repellency to the surface of any material. The CA data, in combination with the SEM analysis, unambiguously demonstrated the vital role played by the coarse

nanostructures of p(PFOMA-*co*-EGDMA) coating in governing the nonwetting property, similar to the nanostructures on rose petals and lotus leaf, creating superhydrophobic surfaces.[18,40] Notably, the high nonwetting ability of p(PFOMA-*co*-EGDMA) coating originated from the co-action of the C6-perfluoroalkyl chains and the surface nanostructures, where the former assisted in lowering the surface free energy the latter contributed to a corrugated surface.

3.4. Mechanical and chemical robustness

Durability against mechanical abrasion and chemical stress is a major challenge for nonwetting coatings. First, the abrasion resistance of the coatings was tested using the Martindale abrasion technique, where a coated substrate is abraded against an abradant. Fig. 6 shows the θ_{water} and $\theta_{dodecane}$ values and morphologies of the coatings before and after 250 cycles of Martindale abrasion. The data show that θ_{water} remained nearly 150°, whereas $\theta_{dodecane}$ decreased to 79.6° (Fig. 6a) for the p(PFOMA-*co*-EGDMA)-coated textile substrate, suggesting the p(PFOMA-*co*-EGDMA) coating to be abrasion-resistant and water-repellent. The coating maintained its texture despite slight degradation by abrasion (Fig. 6b and c). However, after
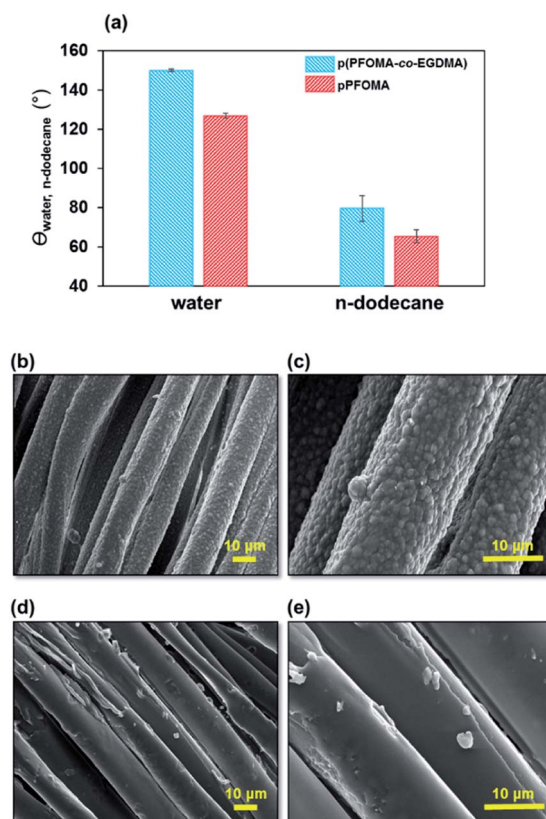

Fig. 6 (a) Effect of Martindale abrasion cycles on the water and *n*-dodecane repellency of the polymeric coatings. SEM images of (b and c) p(PFOMA-*co*-EGDMA) coating and (d and e) the p(PFOMA) coating after 250 Martindale abrasion cycles. The error bars denote standard deviations, obtained from measurements taken at a minimum of three different locations on three different coating samples.

500 cycles of the abrasion test, the nanostructured surface was damaged and the static contact angles of the water and *n*-dodecane droplets decreased: $\theta_{\text{water}} = 118.5°$ and $\theta_{n\text{-dodecane}} = 74.2°$, respectively (Fig. S4†). In the case of p(PFOMA), the degradation after 250 cycles was severe enough to cause a significant loss of nonwetting ability against water and *n*-dodecane as θ_{water} and θ_{dodecane} decreased to 120° and 60°, respectively (Fig. 6a, d and e).

Second, an experiment was conducted with 1 M HCl and 1 M NaOH solutions to assess the chemical resistance. Although such an extremely harsh chemical environment is practically rare, it is nonetheless relevant to establish the chemical robustness of the coatings for CWAs protection fabric.[41] The results showed that the p(PFOMA-*co*-EGDMA) coating maintained a θ_{water} of greater than 120° after 18 h of NaOH and 18 h of HCl exposure (Fig. 7a and b) and a $\theta_{n\text{-dodecane}}$ of greater than 90° after 18 h of NaOH and 4 h of HCl exposure (Fig. 6c and d). The p(PFOMA) coating, however, retained θ_{water} of greater than 90° and $\theta_{n\text{-dodecane}}$ of greater than 70° after 18 h of NaOH and 80° after 4 h of HCl exposure, respectively (Fig. 7a–d). Moreover, the FTIR analysis showed that the characteristic bands of PFOMA clearly remained in the p(PFOMA-*co*-EGDMA) coating, whereas they were noticeably diminished in the case of p(PFOMA) coating (Fig. S5†). Such excellent chemical resistance of p(PFOMA-*co*-EGDMA) could be attributed to crosslinking which enhanced the overall durability.[34]

The above performed experiments confirm that the nonwetting ability generated by the p(PFOMA-*co*-EGDMA) coating on a nylon/cotton fabric shows excellent and very useful qualities. However, any coating is useless if it alters or damage the textile properties in a way that makes it unsuitable for its original purpose. Ideally, the air permeability and tensile strength should be unaffected by the coting. Air permeability measurements performed on the uncoated and the p(PFOMA-*co*-EGDMA) coating according to ISO9237:1995 (ref. 42) reveal that the coating slightly decreased: 6.08 ± 0.04 cm^3 cm^{-2} s^{-1}

p(PFOMA-*co*-EGDMA) coating and 6.47 ± 0.16 cm^3 cm^{-2} s^{-1}, uncoated (Fig. S6†).

Tensile strength measurements were performed on the uncoated and p(PFOMA-*co*-EGDMA) coating according to KS K0520:2015 (ref. 43) and reveal that the coating can improve the fabric strengths: from 650 N (warp)/430 N (weft), uncoated to 720 N (warp)/480 N (weft), the p(PFOMA-*co*-EGDMA) coating (Fig. S7†). This characteristic is ascribed to the p(PFOMA-*co*-EGDMA) layer which was strongly adhered to the skeleton of the fabric.

Finally, the p(PFOMA-*co*-EGDMA) coating was analysed if there are residual amounts of PFOA and PFOS present in the coating materials in accordance with CEN/TS 15968:2014.[44] For comparison, the C8-based coating currently in use for military fabrics was compared as well. The results show that while the level of 6.6 µg m^{-2} of PFOA was detected in the C8-based coating, both PFOA and PFOS were undetectable in the p(PFOMA-*co*-EGDMA) coating, suggesting that our coating materials are relatively less toxic and, accordingly, are safer for military applications.

4. Conclusions

To provide the military personnel with better integrated CWAs protective fabric properties, p(PFOMA-*co*-EGDMA)-coated textile with excellent nonwetting ability against CWAs, water, and *n*-dodecane were prepared. It is worth emphasizing that the highest CA values of GD and VX nerve agents were obtained in this study. Due to the inherent hydrophobicity of the fluorine-based PFOMA and nanostructured morphology, the p(PFOMA-*co*-EGDMA) coating was significantly robust against mechanical abrasion and harsh chemical environments. Interestingly, the application of such outstanding nonwetting coating to CWAs protection fabric could offer added trade space, such as noticeably enhanced chemical protection while posing virtually no hindrance to air and moisture vapors when conformally coated onto thin, lightweight, and tightly woven textiles. Additionally, these nonwetting coated textiles that resist the incursion of CWAs could significantly extend the protection performance duration of the clothing.

Author contributions

Hyunsook Jung: conceptualization, investigation, visualization, experiment, data curation, writing–original draft. Jihyun Kwon: conceptualization, experiment, validation, writing–review & editing. Heesoo Jung: conceptualization, investigation, methodology, writing–review & editing. Kyeong Min Cho: experiment, writing–review & editing. Seung Jung Yu: experiment, validation, writing–review & editing. Sang Myeon Lee: writing–review & editing. Mingyu Jeon: experiment. Sung Gap Im: methodology, writing–review & editing.

Conflicts of interest

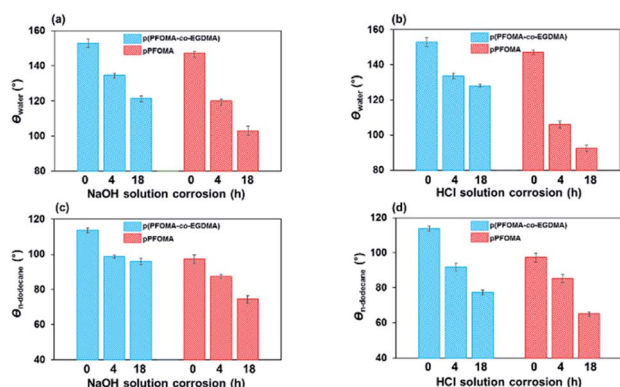There are no conflicts to declare.

Fig. 7 The effect of NaOH solution exposure on nonwetting properties toward (a) water and (b) *n*-dodecane. The effect of HCl solution exposure on nonwetting properties toward (c) water and (d) *n*-dodecane. The error bars denote standard deviations, obtained from measurements taken at a minimum of three different locations on three different coating samples.

Acknowledgements

Notes and references

1 Organization for the Prohibition of Chemical Weapons. Convention on the Prohibition of the development, Production, Stockpiling and Use of Chemical Weapons and on Their Destruction see: http://www.opcw.nl.

2 A. M. Coclite, R. M. Howden, D. C. Borrelli, C. D. Petruczok, R. Yang, J. L. Yagüe, A. Ugur, N. Chen, S. Lee, W. J. Jo, A. Liu, X. Wang and K. K. Gleason, *Adv. Mater.*, 2013, **25**, 5392–5423.

3 H. Götz, F. Bauers and W. Knaup, *US Pat.* 7976583, 2011.

4 S. Schellenberger, P. J. Hill, O. Levenstam, P. Gillgard, I. T. Cousins, M. Taylor and R. S. Blackburn, *J. Cleaner Prod.*, 2019, **217**, 134–143.

5 Q. Truong, B. Koene, J. Domino, *NSTI-Nanotech*, 2013, ISBN 978-1-4822-0581-7, vol. 1, pp. 663–666.

6 Q. Truong and N. Pomerantz, *Military applications: Development of superomniphobic coatings, textiles and surfaces*, Woodhead Publishing, Cambridge, MA, 2018, pp. 473–531.

7 K. Prevedouros, I. T. Cousins, R. C. Buck and S. H. Korzeniowski, *Environ. Sci. Technol.*, 2006, **40**, 32–44.

8 J. M. Conder, R. A. Hoke, W. D. Wolf, M. H. Russell and R. C. Buck, *Environ. Sci. Technol.*, 2008, **42**, 995–1003.

9 European Union, *OJEU 372, Directive 2006/122/EC of the European Parliament and of the Council of 12 December 2006 amending for the 30th time Council Directive 76/769/EEC on the approximation of the laws, regulations and administrative provisions of the member states relating to restrictions on the marketing and use of certain dangerous substances and preparations (perfluorooctane sulfonates)*, 2006, pp. 32–34.

10 United States Environmental Protection Agency, 2006. Docket ID: EPA-HQ-OPPT-2006–0621.

11 J. S. Bowman, *Environ. Health Perspect.*, 2015, **123**, A112.

12 H. Götz, F. Bauers and W. Knaup, WO 2008/022985 A1, PCT/EP2007/058620, 2008.

13 D. Soto, A. Ugur, T. A. Farnham, K. K. Gleason and K. K. Varanasi, *Adv. Funct. Mater.*, 2018, **28**, 1707355.

14 Q. Zhang, Q. Wang, J. Jiang, Z. Zhan and F. Chen, *Langmuir*, 2015, **31**, 4752–4760.

15 C. M. Grozea, *RMCC CPT-1802*, DRDC-Suffield Research Centre, 2018.

16 K. Bryan, *US Pat.*, 2013/0109261 A1, 2013.

17 Q. Truong, W. Zukas, E. A. Welsh, P. Stenhous, P. Brown, N. Hoffman, J. Mead, C. Barry, P. Mooney, B. Koene, M. Slaughter, R. Cohen, G. McKinley and D. Chen, *TechConnect Briefs*, TechConnect.org, ISBN 978-0-9975-1170-3, 2016, pp. 272–275.

18 R. Campos, A. J. Guenthner, T. S. Haddad and J. M. Mabry, *Langmuir*, 2011, **27**, 10206–10215.

19 R. Hensel, C. Neinhuis and C. Werner, *Chem. Soc. Rev.*, 2016, **45**, 323–341.

20 H. Jung, M.-k. Kim and S. Jang, *J. Colloid Interface Sci.*, 2020, **563**, 363–369.

21 W. Ming, D. Wu, R. van Benthem and G. de With, *Nano Lett.*, 2005, **5**, 2298–2301.

22 T. Sun, L. Feng, X. Gao and L. Jiang, *Acc. Chem. Res.*, 2005, **38**, 644–652.

23 A. Tuteja, W. Choi, M. L. Ma, J. M. Mabry, S. A. Mazzella, G. C. Rutledge, G. H. McKinley and R. E. Cohen, *Science*, 2007, **318**, 1618–1622.

24 G. Zhang, S. Lin, I. Wyman, H. Zou, J. Hu, G. Liu, J. Wang, F. Li, F. Liu and M. Hu, *ACS Appl. Mater. Interfaces*, 2013, **5**, 13466–13477.

25 J. Kwon, H. Jung, H. Jung and J. Lee, *Polymers*, 2020, **12**, 1826.

26 A. Liu, E. Goktekin and K. K. Gleason, *Langmuir*, 2017, **30**, 14189–14194.

27 W. E. Tenhaeff and K. K. Gleason, *Adv. Funct. Mater.*, 2008, **18**, 979–992.

28 S. J. Yu, K. Pak, M. J. Kwak, M. Joo, B. J. Kim, M. S. Oh, J. Baek, H. Park, G. Choi, D. H. Kim, J. Choi, Y. Choi, J. Shin, H. Moon, E. Lee and S. G. Im, *Adv. Eng. Mater.*, 2018, **20**, 1700622.

29 F. Bai, X. Yang, R. Li, B. Huang and W. Huang, *Polymer*, 2006, **47**, 5775–5784.

30 P. Christian and A. M. Coclite, *Beilstein J. Nanotechnol.*, 2017, **8**, 933–942.

31 J. Zimmermann, S. Seeger and F. A. Reifler, *Text. Res. J.*, 2009, **79**, 1565–1570.

32 X. Wang, X. Liu and C. H. Deakin, *Fabric testing: 4-Physical and mechanical testing of textiles*, Woodhead Publishing, ISBN 978-1-84569-298-1, 2008, pp. 90–124.

33 Y. Mao and K. K. Gleason, *Langmuir*, 2004, **20**, 2484–2488.

34 K. K. Gleason, *Front. Bioeng. Biotechnol.*, 2021, **9**, 632753.

35 I. Vilaró, J. L. Yagüe and S. Borrós, *ACS Appl. Mater. Interfaces*, 2017, **9**, 1057–1065.

36 M. Gupta and K. K. Gleason, *Langmuir*, 2006, **22**, 10047–10052.

37 J. Zimmermann, F. A. Reifler, L.-C. Gerhardt and S. Seeger, *Adv. Funct. Mater.*, 2008, **18**, 3662–3669.

38 T. Liu and C.-J. Kim, *Science*, 2014, **346**, 1096–1100.

39 D. Kim, H. Im, M. J. Kwak, E. Byun, S. G. Im and Y.-K. Choi, *Sci. Rep.*, 2016, **6**, 29993.

40 S. Das, S. Kumar, S. K. Samal, S. Mohanty and S. K. Nayak, *Ind. Eng. Chem. Res.*, 2018, **57**, 2727–2745.

41 C. Peng, Z. Chen and M. K. Tiwari, *Nat. Mater.*, 2018, **17**, 355–360.

42 ISO 9237:1995. Textiles – Determination of the permeability of fabrics to air.

43 KS K 0520:2015. Textiles – Tensile properties of fabrics – Determination of maximum force and elongation at maximum force using the gram method.

44 CEN/TS 15968:2014. Determination of extractable perfluorooctanesulfonate (PFOS) in coated and impregnated solid articles, liquids and fire fighting foams – Method for sampling, extraction and detection by LC-MS/MS or LC-MS.